Supplementary Information

Multicomponent Nanomaterials with Complex Networked Architectures from Orthogonal Degradation and Binary Metal Backfilling in ABC Triblock Terpolymers

Christina D. Cowman,[1] Elliot Padgett,[2] Kwan Wee Tan,[3] Robert Hovden,[2] Yibei Gu,[3] Nina Andrejevic,[2] David Muller,[2] Geoffrey W. Coates,*[1] and Ulrich Wiesner*[3]

[1]*Department of Chemistry and Chemical Biology, Baker Laboratory, Cornell University, Ithaca, NY 14853*

[2]*Department of Applied and Engineering Physics, Clark Hall, Cornell University, Ithaca, NY 14853*

[3]*Department of Materials Science and Engineering, Bard Hall, Cornell University, Ithaca, NY 14853*

General Considerations

Handling of air and water-sensitive compounds was carried out in either a Braun Labmaster nitrogen glovebox or using standard Schlenk techniques.

^{1}H NMR spectroscopy was carried out using an INOVA 400 MHz spectrometer with d-chloroform as a solvent (n = 8, d_1 = 10 s, PW = 45). Gel-permeation chromatography (GPC) was carried out with an Agilent PL-GPC50 instrument with THF as an eluent at 30 °C and a flow rate of 0.3 mL/min. The GPC was outfitted with two PL Mini-MIX C columns. The data shown was from an RI detector. The GPC was calibrated using monodisperse polystyrene samples.

Small-angle X-ray scattering (SAXS) analysis was performed on bulk polymer films at the G1 line of the Cornell High Energy Synchrotron Source (CHESS). Measurements were taken at a path length of 6 m with a beam energy of 10.05 keV. The two-dimensional patterns obtained from a point-collimated beam were azimuthally integrated to yield the one-dimensional plots shown in the Supporting Information Figures S6 and S7.

Samples were prepared for transmission electron microscopy (TEM) by sectioning using a Leica UCT cryo-ultramicrotome at -65 °C. Samples were cut to a final thickness of 70–100 nm. TEM micrographs were taken using a Technai T12 TEM operating at 120 kV.

SEM micrographs were taken using a LEO-1550 scanning electron microscope operating at 2 kV with in-lens and Everhart-Thornley detectors. The STEM images were acquired on a FEI Tecnai F20 with a Schottky field emission gun operating at 200 kV.

Chemicals

Isoprene (99%), styrene (99%), *sec*-butyllithium (1.4 M in cyclohexane), and ethylene oxide (>99.5%) were obtained from Sigma-Aldrich. *n*-Butyllithium (1.6 M in hexanes) was obtained from Acros. Isoprene was dried using *n*-butyllithium, distilled, and transferred to a nitrogen glovebox prior to use. Styrene was dried for 16 hours over calcium hydride, degassed using three freeze-pump-thaw cycles, distilled, and transferred to a glovebox before use. Propylene oxide (*rac*, >99%) was obtained from Sigma-Aldrich, dried for three days over calcium hydride, degassed using three freeze-pump-thaw cycles, transferred under reduced pressure, and stored in a glovebox. Research-grade carbon dioxide was obtained from Airgas and dried over activated 3Å molecular sieves prior to use. Other solvents (*e.g.* dichloromethane, methanol, ethanol) were used as received. Polymer films were always cast using HPLC-grade THF. Bis(triphenylphosphine)iminium chloride [[PPN]Cl] was purchased from Sigma-Aldrich and purified according to previous literature procedures.[1]

Nickel (II) sulfate heptahydrate (≥99%), copper (II) sulfate pentahydrate (99.995%), ethylenediaminotetraacetic acid (EDTA) (99.4%), borane dimethylamine complex (DMAB) (97%), sodium citrate dihydrate (≥99%), lactic acid (85% solution in water), diethanolamine (≥99.5%), triethanolamine (≥99.0%), gold(III) chloride trihydrate (99.9%), tin(II) chloride(98%), and palladium (II) chloride (99%) were obtained from Sigma-Aldrich and used as received. Sodium borohydride (98%) was obtained from Acros and used as received.

PI-*b*-PS-OH diblock copolymer synthesis

Hydroxy-terminated polyisoprene-*b*-polystyrene (PI-*b*-PS-OH) was synthesized according to previous literature procedures.[2] Trace water was removed from PI-*b*-PS-OH by dissolving the polymer in dichloromethane and removing the solvents under reduced pressure at 85 °C over activated Drierite. Anhydrous PI-*b*-PS-OH was stored in a nitrogen glovebox prior to use.

Scanning electron microscopy (SEM)

Porous polymer samples were prepared for scanning electron microscopy (SEM) by mounting polymer films onto carbon tape and coating with a 1-2 nm layer of Au/Pd to prevent charging. Samples were coated using a Denton Vacuum Desk II sputter coater.

SEM micrographs of inorganic samples were taken by plasma cleaning sectioned samples of polymer-inorganic hybrids for 30 minutes to remove organic material and leave free-standing inorganic networks. Organic material from Cu-containing hybrid materials was removed by dissolution in THF for one hour. Samples were plasma cleaned with a Harrick plasma cleaner with air plasma. Inorganic networks with organic material removed can withstand higher SEM operating voltages of 5 kV without charging and did not require coating with Pd/Au prior to imaging.

Scanning transmission electron microscopy (STEM)

The STEM images were acquired on a FEI Tecnai F20 with a Schottky field emission gun operating at 200 kV. A convergence angle of ~6.9 mrad was used for optimal tradeoff between resolution and depth of field. A high-angle annular dark field (HAADF)

detector at a camera length of 100 mm was used, providing incoherent projection images with a signal proportional to the material thickness and to $Z^{1.7}$. A STEM image tilt series was acquired with 1.5° increments ranging from -74° to +74°. The tilt series was manually aligned and reconstructed using custom software written in Matlab. The reconstruction was generated using the simultaneous iterative reconstruction technique (SIRT) with 25 iterations. Visualizations were created using Avizo 8.1. STEM simulations were calculated from perfect projections of material structures with uniform density.[3]

Characterization of PI-*b*-PS-*b*-PPC triblock terpolymers

Composition of PI-*b*-PS-*b*-PPC triblock terpolymers was determined using ^{1}H NMR spectroscopy and GPC. A ^{1}H NMR spectrum of PI-*b*-PS-*b*-PPC (entry 4, Table 1 from the main text) is shown in Figure S1. ^{1}H NMR assignments are as follows: δ 7.07 (PS, Ar-*H*, 3H), δ 6.57 (PS, Ar-*H*, 2H), δ 5.13 (PI, C=C-*H*, 1H), δ 5.01 (PPC, -C*H*-, 1 H), δ 4.72 (PI, 3,4 PI, 2H), δ 4.20 (PPC, -CH_2-, 2 H). GPC traces of PI-*b*-PS-*b*-PPC terpolymers from Table 1 in the main text are shown in Figures S2-S5.

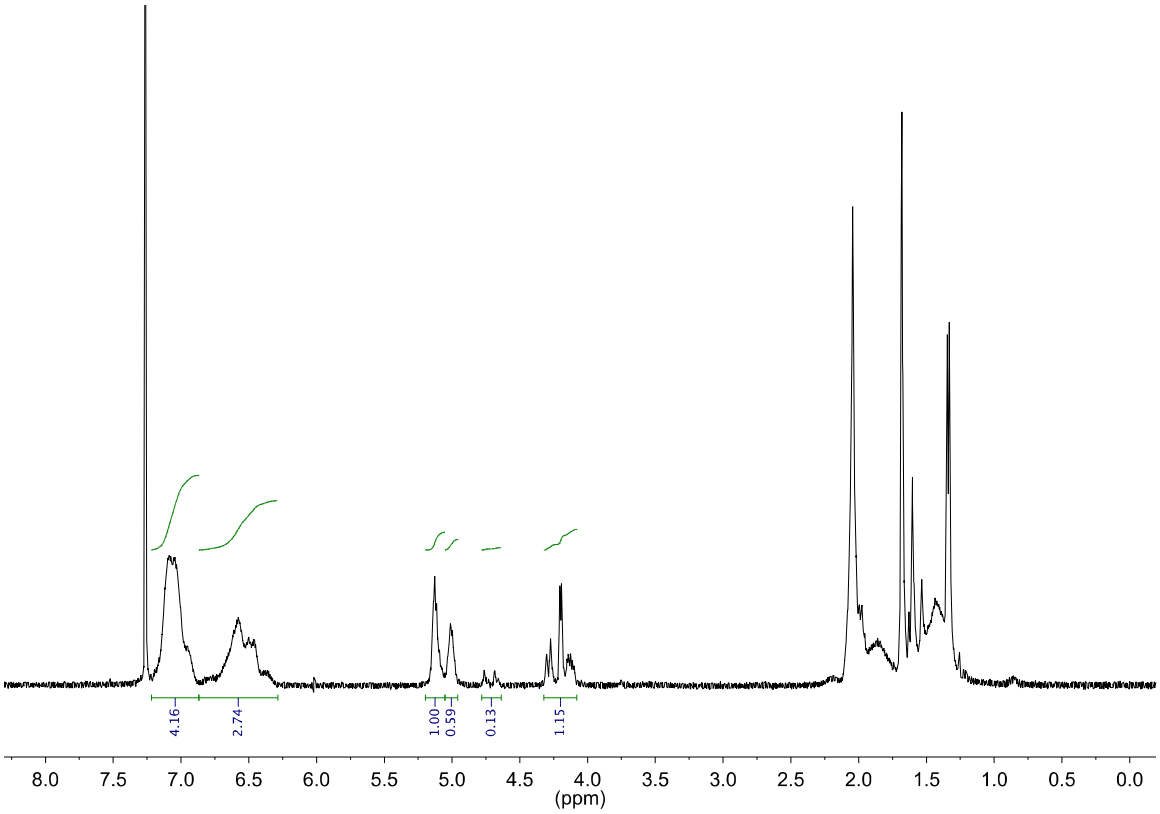

Figure S1. ^{1}H NMR spectrum of PI-*b*-PS-*b*-PPC-4 (entry 4, Table 1). in $CDCl_3$ (400 MHz, n = 8, d_1 = 10s, PW = 45).

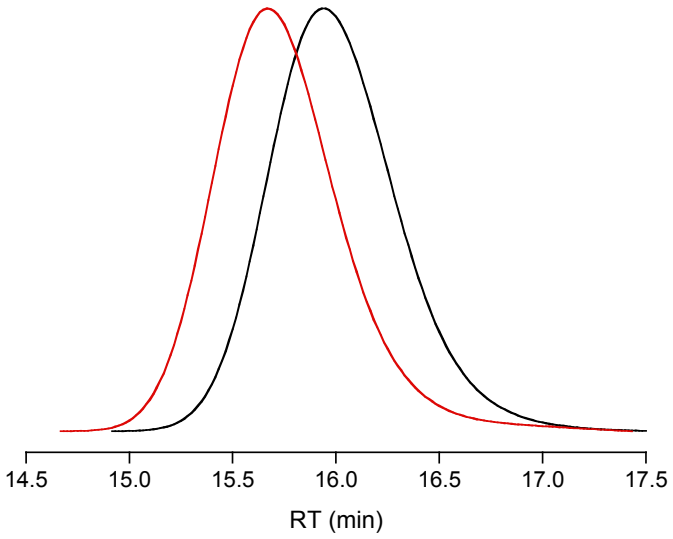

Figure S2. GPC traces of PI-*b*-PS-*b*-PPC-1 (Table 1, red) and parent PI-*b*-PS-OH diblock copolymer (black).

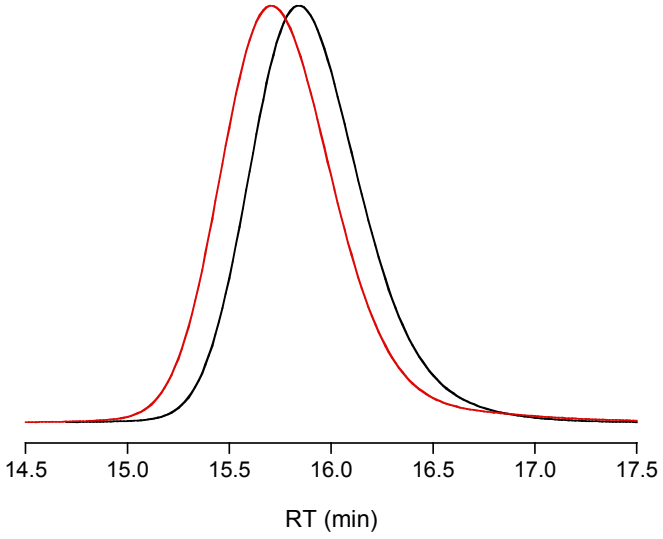

Figure S3. GPC traces of PI-*b*-PS-*b*-PPC-2 (Table 1, red) and parent PI-*b*-PS-OH diblock copolymer (black).

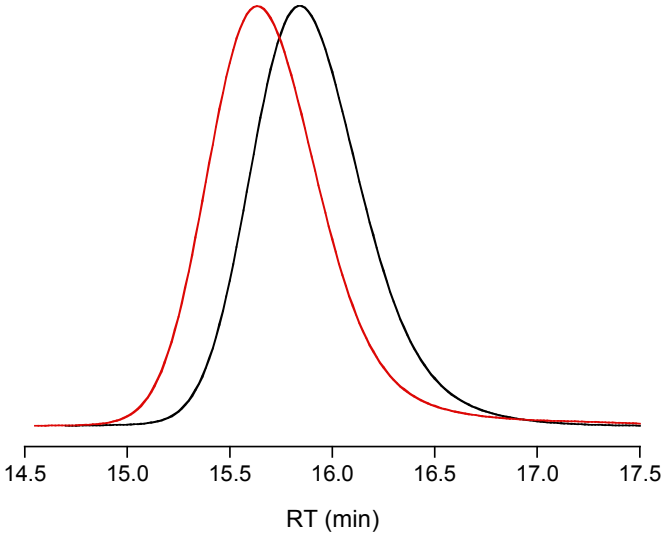

Figure S4. GPC traces of PI-*b*-PS-*b*-PPC-3 (Table 1, red) and parent PI-*b*-PS-OH diblock copolymer (black).

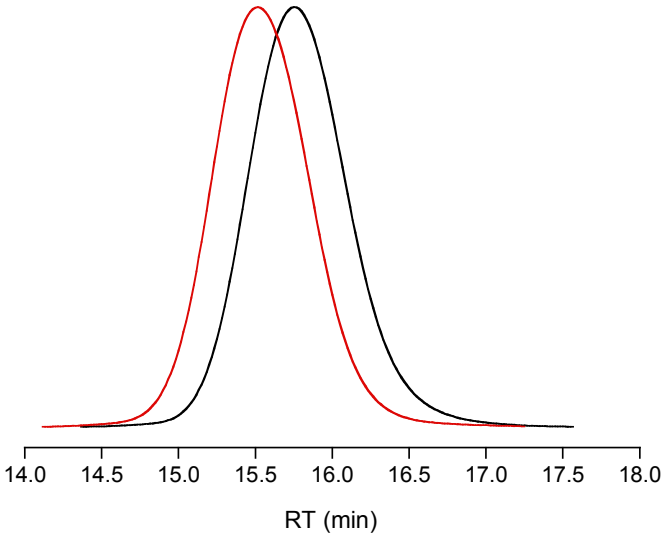

Figure S5. GPC traces of PI-*b*-PS-*b*-PPC-4 (Table 1, red) and parent PI-*b*-PS-OH diblock copolymer (black).

Volume fraction of each block was determined by calculating the weight fraction of each block and dividing by the density. Densities of 0.904 g/mL,[2] 1.05 g/mL,[2] and 1.26 g/mL[4] were used for PI, PS, and PPC, respectively.

Morphologies were characterized by a combination of SAXS and TEM. SAXS patterns for all polymers from Table 1 are found in Figure S6 in a stack plot. Patterns for PI-*b*-PS-*b*-PPC terpolymers 3 and 4 are consistent a core-shell double gyroid structure (space group Q^{230}) with peaks indexed with expected reflections of $6^{½}$, $8^{½}$, $14^{½}$, $16^{½}$, etc. relative to the forbidden first order (100) peak.[5] The SAXS pattern of PI-*b*-PS-*b*-PPC-2 is indexed with the expected reflections for an alternating gyroid structure (space group Q^{214}) with expected reflections of $2^{½}$, $6^{½}$, $8^{½}$, $10^{½}$, etc. relative to the forbidden first order (100) peak.[6] The SAXS results for PI-*b*-PS-*b*-PPC-1 did not fit to any of the classical block copolymer morphologies. A higher resolution reproduction of this pattern is shown in Figure S7 with expected peak positions for an orthorhombic lattice with the *Fddd* space group O^{70} and lattice parameters of a = 33.9 nm, b = 49.4 nm, and c = 82.1 nm, which provided the best fit.[7] Examples of representative TEM or SEM micrographs consistent with the network structures of the various PI-*b*-PS-*b*-PPC terpolymers from Table 1 are shown in Figures 2-5 from the main text in addition to Figure S8.

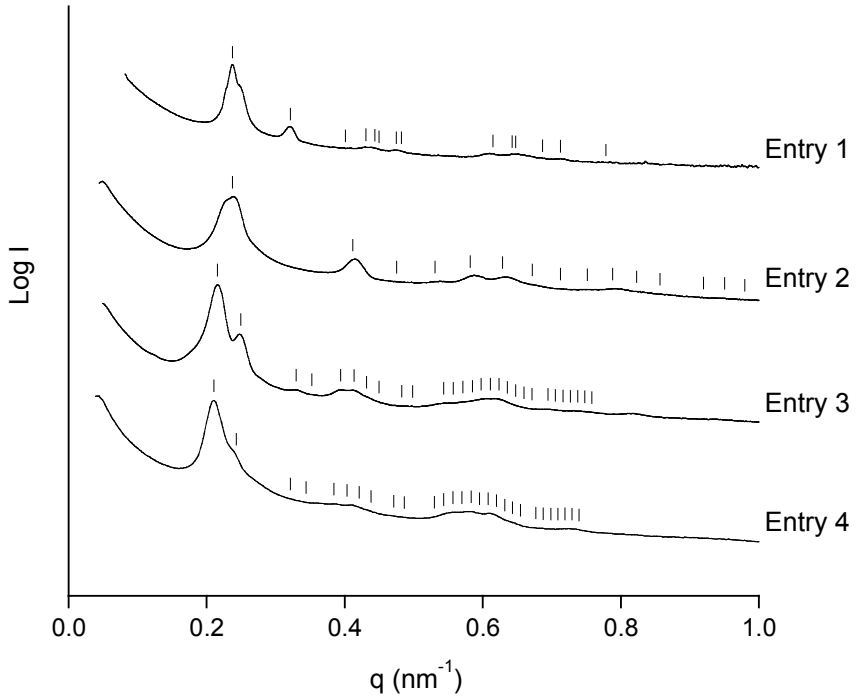

Figure S6. SAXS patterns of self-assembled PI-*b*-PS-*b*-PPC triblock terpolymers from Table 1. Patterns are shifted vertically. Expected reflections for each network structure are indicated by ticks.

Peak assignments for PI-*b*-PS-*b*-PPC-1 are shown in Figure S7. The SAXS pattern for PI-*b*-PS-*b*-PPC-1 is fit with an orthorhombic lattice and an *Fddd* space group with lattice parameters a = 33.9 nm, b = 49.4 nm, c = 82.1 nm (O^{70}).[7]

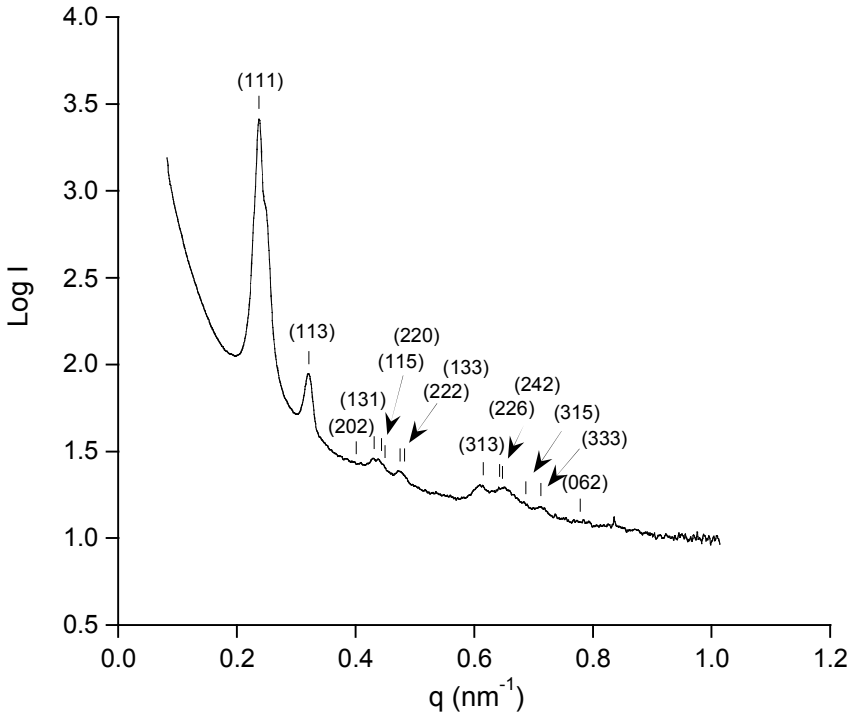

Figure S7. SAXS pattern for PI-*b*-PS-*b*-PPC-1. Pattern is indexed with an orthorhombic lattice with *Fddd* symmetry (a = 33.9 nm, b = 49.4 nm, c = 82.1 nm). Reflections are indicated with dashes and assignments are indicated.

Representative TEM micrographs for network-structured PI-*b*-PS-*b*-PPC-3 from Table 1 are shown in Figure S8. The polyisoprene domains were selectively stained dark with OsO_4 vapor to provide contrast. The TEM micrographs from Figure S8a and Figure S8b are consistent with the (111) projection and (211) projections, respectively, of the Q^{230} core-shell double gyroid.[5]

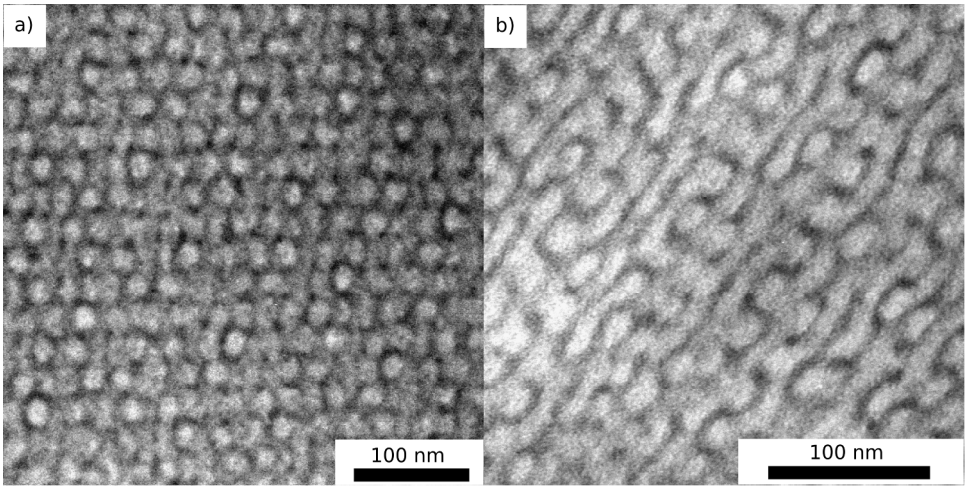

Figure S8. TEM micrographs for PI-*b*-PS-*b*-PPC-3 from Table 1. Polyisoprene domains are selectively stained dark with OsO_4.

Film casting procedure

PI-*b*-PS-*b*-PPC films were cast from a 1.3 wt% solution of HPLC-grade THF in a 1.25" Teflon pan (16 mg PI-*b*-PS-*b*-PPC, 1.2 g THF) covered with a glass dish. A vial with 1-2 mL of THF was placed next to the Teflon pan during solution casting to slow down the rate of solvent evaporation. The final thicknesses of the films were between 20-30 μm. Humidity can affect the film morphologies formed by the PI-*b*-PS-*b*-PPC terpolymers during solvent casting. Casting films under a blanket of nitrogen and using anhydrous solvent was sufficient to prevent problems with structure formation due to humidity.

Orthogonal degradation of PI-*b*-PS-*b*-PPC films

^{1}H NMR spectra of polymer films after different degradation steps were taken using films of PI-b-PS-b-PPC-3. A ^{1}H NMR spectrum of a PI-*b*-PS-*b*-PPC film after 302 nm UV light treatment to selectively degrade the PI block is shown in Figure S9. A ^{1}H NMR spectrum of a PI-*b*-PS-*b*-PPC film after 302 nm UV light treatment to selectively degrade the PI block followed by NaOH treatment to selectively degrade the PPC block is shown in Figure S10. A ^{1}H NMR spectrum of a PI-*b*-PS-*b*-PPC film after NaOH treatment to selectively degrade the PPC block is shown in Figure S11. A ^{1}H NMR spectrum of a PI-*b*-PS-*b*-PPC film after NaOH treatment to selectively degrade the PPC block followed by 302 nm UV light treatment to selectively degrade the PI block is shown in Figure S12. Signals at δ 6.57 (PS, Ar-*H*, 2H) and δ 7.07 (PS, Ar-*H*, 3H) are indicative of the non-labile PS. Spectra are noisy due to small amounts of material available for ^{1}H NMR spectroscopy.

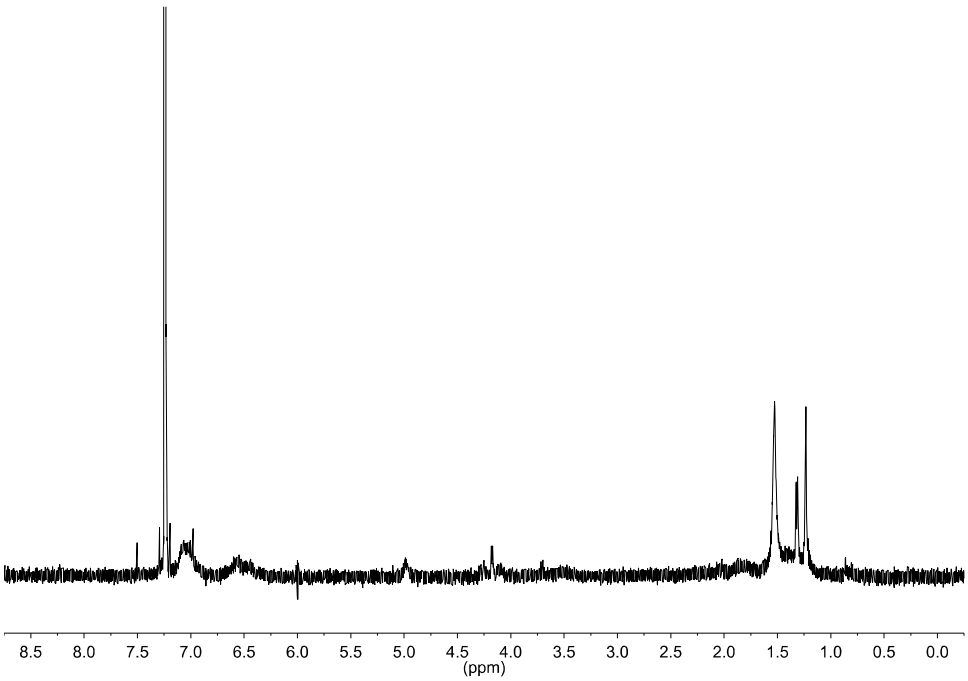

Figure S9. ^{1}H NMR spectrum taken in $CDCl_3$ (n = 8, d_1= 10s, PW = 45) of re-dissolved PI-*b*-PS-*b*-PPC after film degradation with 302 nm UV light to selectively degrade the PI block.

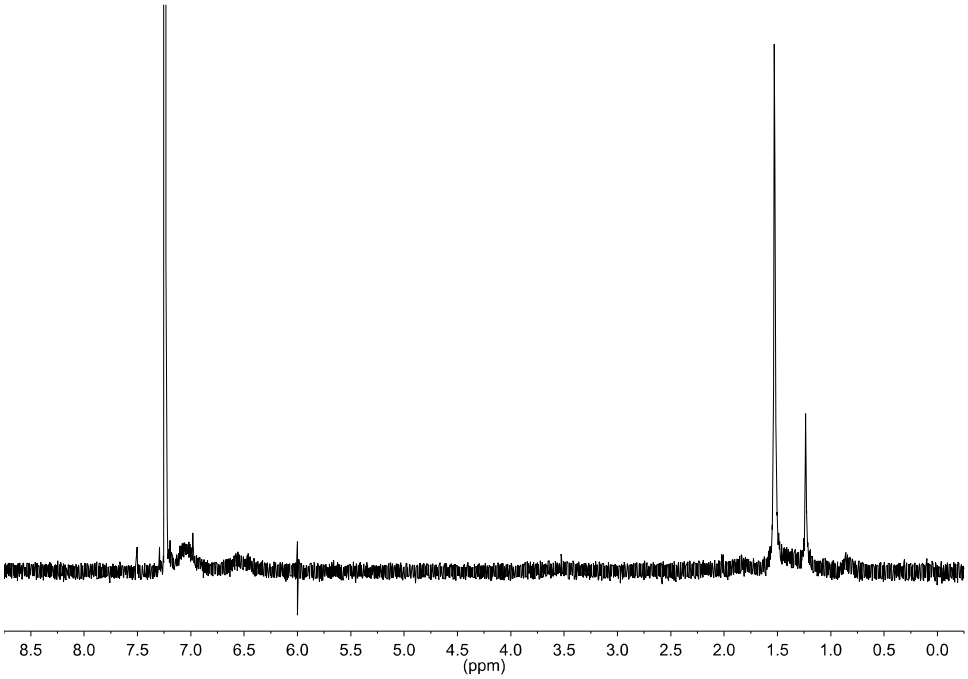

Figure S10. ^{1}H NMR spectrum of re-dissolved PI-*b*-PS-*b*-PPC after film degradation with 302 nm UV light to selectively degrade the PI block followed by treatment with NaOH to selectively degrade the PPC block. Spectrum was taken in $CDCl_3$ (n = 8, d_1 = 10s, PW = 45).

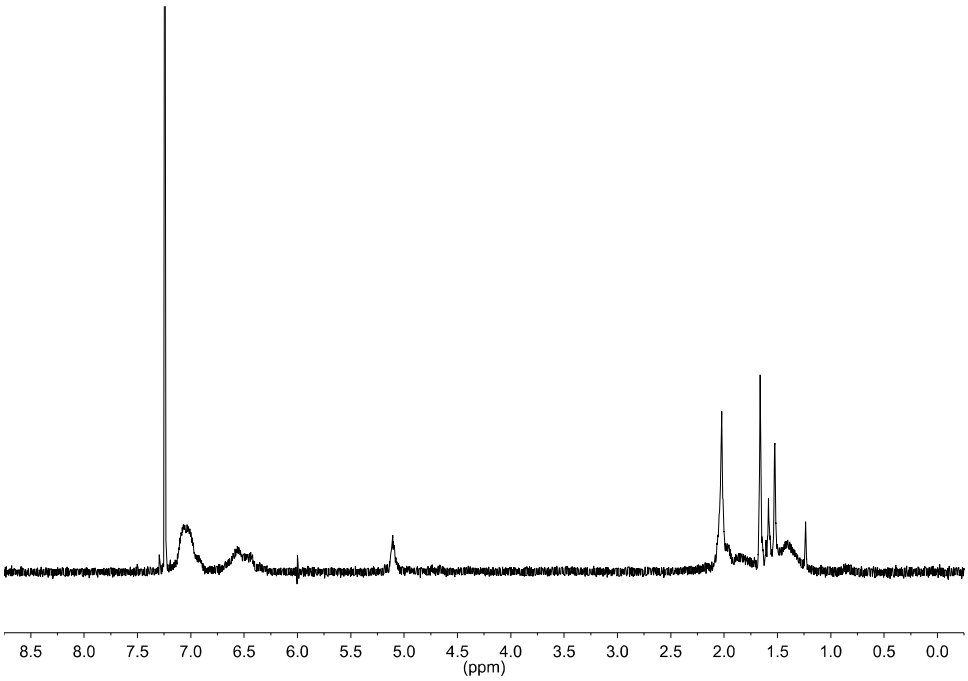

Figure S11. ^{1}H NMR spectrum of re-dissolved PI-*b*-PS-*b*-PPC after film treatment with NaOH to selectively remove the PPC block. Spectrum was taken in $CDCl_3$ (n = 8, d_1 = 10s, PW = 45).

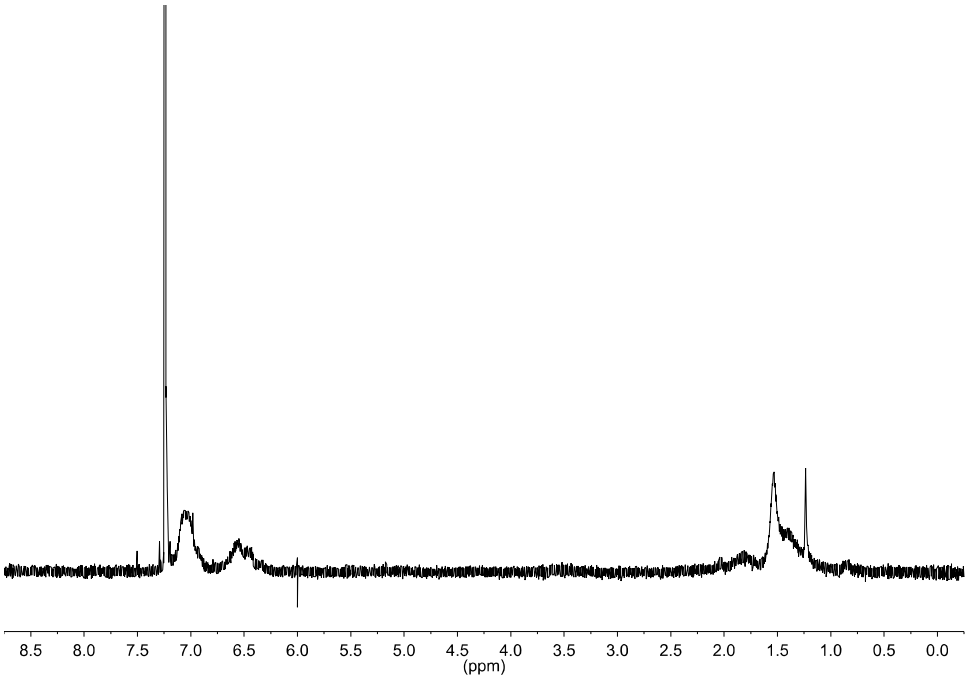

Figure S12. ^{1}H NMR spectrum of re-dissolved PI-*b*-PS-*b*-PPC after film treatment with NaOH to selectively remove the PPC block followed by treatment with 302 nm UV light to selectively degrade the PI block. Spectrum was taken in $CDCl_3$ (n = 8, d_1 = 10s, PW = 45).

Figure S13a shows an example of a low-magnification SEM micrograph of a large-area PI-*b*-PS-*b*-PPC-3 film cross-section after degradation of the PI block with 302 nm UV light. SEM micrographs of film surfaces after degradation of the PI block (PI-*b*-PS-*b*-PPC-3, Figure S13b) and PPC block (PI-*b*-PS-*b*-PPC-1, Figure S13c) show film surface porosity.

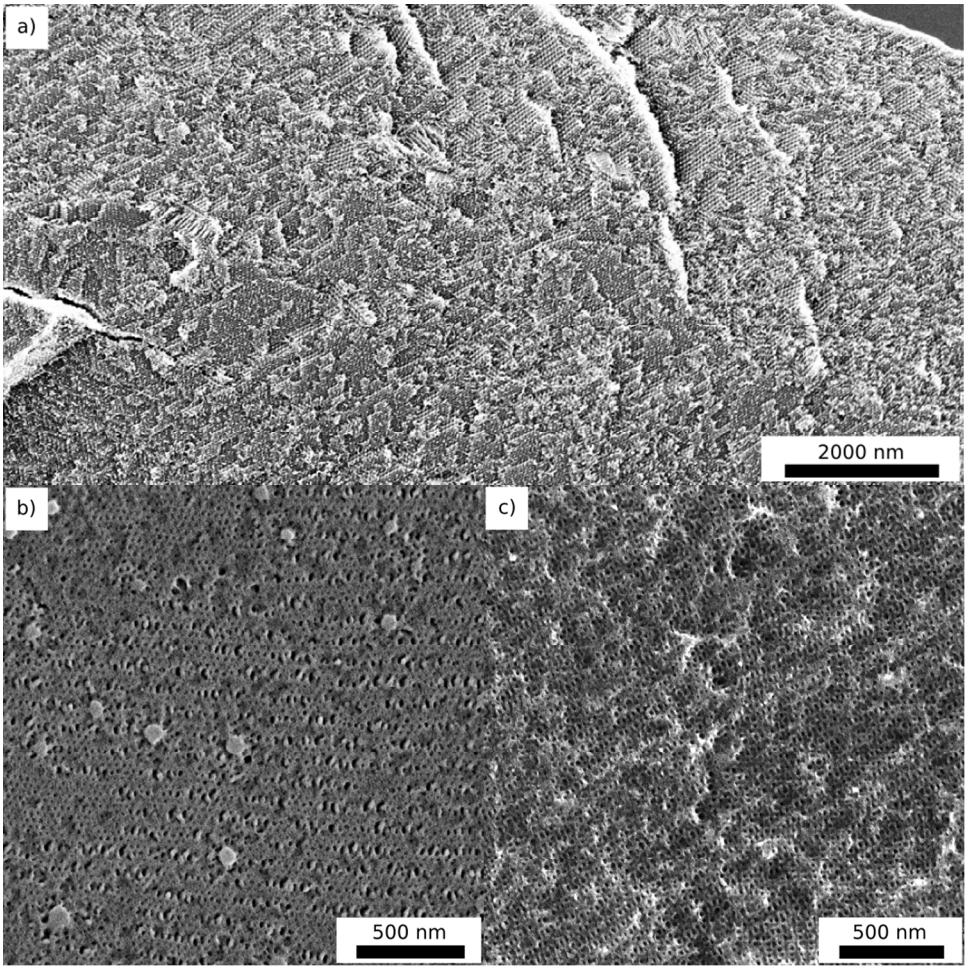

Figure S13. SEM micrographs of large-area polymer film cross-sections and surfaces after degradation. (**a**) Large-area SEM micrograph of PI-*b*-PS-*b*-PPC-3 film cross-section after degradation of PI blocks. (**b,c**) SEM micrographs of polymer film surfaces after: (**b**) Degradation of PI blocks (PI-*b*-PS-*b*-PPC-3) and (**c**) degradation of PPC blocks (PI-*b*-PS-*b*-PPC-1).

Electroless deposition into block copolymer templates

Deposition of Au-metal. Au-metal was deposited into gyroidal mesopores using a protocol adapted from one by Hsueh *et al.*[8] All Au deposition steps were performed at 21

°C. Mesoporous polymer templates were soaked for 3-4 hours in an Au-seeding bath solution consisting of 50 ppm $HAuCl_4$ in methanol. Polymer films were removed from the $HAuCl_4$ seeding solution and soaked for 5 minutes in methanol to remove surface Au^{3+} ions. The polymer films were then transferred to a reducing solution of 0.025 M sodium borohydride in methanol for 20 minutes, nucleating Au nanoparticles inside the confines of the mesopores.[8] The films containing Au particles were soaked in methanol for 5 minutes to remove any Au ions or particles from the film surface. The seeded films were transferred to an Au growth solution of 6.3 mM $HAuCl_4$ trihydrate, 47.5 mM diethanolamine, and 5 mM HCl in methanol for 72 hours. The Au growth solution was replaced after 48 hours to prevent solution decomposition.

Electroless deposition of Cu-metal. Mesoporous polymer films were sensitized for electroless deposition using a 0.1 M solution of tin(II) chloride in 0.1 M HCl for 4 hours at 21 °C under nitrogen. The polymer films were then rinsed with DI water and transferred into a palladium-based catalyzing solution of 6.5 mM solution of palladium (II) chloride in a 90:10 ethanol : 1 M HCl mixture by volume at 21 °C for 48 hours. Note: the palladium solution takes around 2 hours to fully dissolve during preparation.

The catalyzed films were rinsed using DI water and transferred into a Cu electroless plating solution[9] consisting of 12 mM copper sulfate, 35 mM EDTA as a complexing agent, 0.38 M triethanolamine as a stabilizer, and 15 mM DMAB as a reducing agent in water. The plating solution was buffered to pH 7.5 using concentrated phosphoric acid. The films were plated at 4 °C for 24 hours. After plating the films were washed with DI

water and dried under reduced pressure. Cu-plated films are copper-colored due to overgrowth of Cu-metal on the film surface.

Electroless deposition of Ni-metal. Mesoporous polymer films were sensitized for electroless deposition using a 0.1 M solution of tin(II) chloride in 0.1 M HCl for 4 hours at 21 °C under nitrogen. The polymer films were then rinsed with DI water and transferred into a palladium-based catalyzing solution of 6.5 mM solution of palladium (II) chloride in a 90:10 mixture of ethanol : 1 M HCl by volume at 21 °C for 48 hours. Note: the palladium solution takes around 2 hours to fully dissolve during preparation.

The catalyzed films were rinsed using DI water and transferred into a Ni electroless plating solution consisting of 13 mM nickel(II) sulfate heptahydrate, 78 mM sodium citrate dihydrate as a complexing agent, 0.13 M lactic acid as a stabilizer, and 18 mM DMAB as a reducing agent in water. The plating solution was buffered to pH 7 using concentrated ammonium hydroxide. The films were plated at 4 °C for 24 hours. After plating the films were washed with DI water and dried under reduced pressure. Ni-plated films are gray due to overgrowth of Ni metal on the film surface.[10]

SEM micrographs of Au and Ni gyroid networks

A SEM micrograph of Au gyroid networks deposited into the PI matrix pores of PI-*b*-PS-*b*-PPC-4 after removal of the remaining organic material with air plasma is shown in Figure S14.

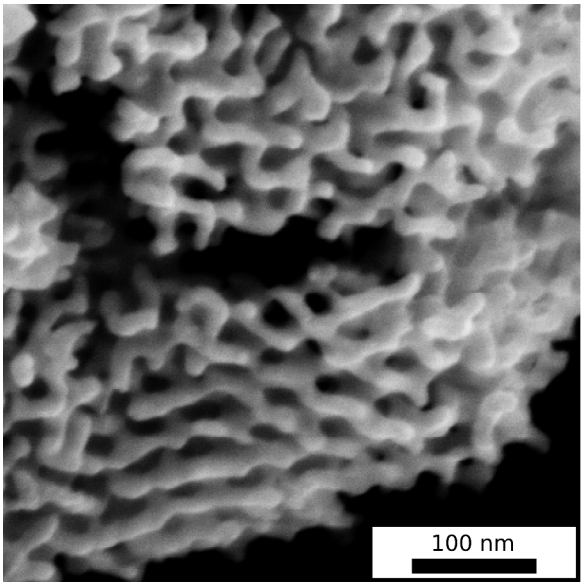

Figure S14. SEM micrograph of Au deposited into the matrix PI pores of PI-*b*-PS-*b*-PPC-4 (Q^{230} core-shell double gyroid).

A SEM micrograph of Ni metal deposited into the PI matrix pores of the Q^{230} core-shell double gyroid structure of PI-*b*-PS-*b*-PPC-4 is shown in Figure S15. A SEM micrograph of Ni metal deposited into the PPC minority network pores of the O^{70} structure of PI-*b*-PS-*b*-PPC-1 is shown in Figure S16. Remaining polymer was removed from the hybrids in Figures S15 and S16 by plasma cleaning for 30 minutes with air plasma in 10-minute intervals with 3-min breaks for the samples to cool. The SEM micrographs were taken with an operating voltage of 2 kV.

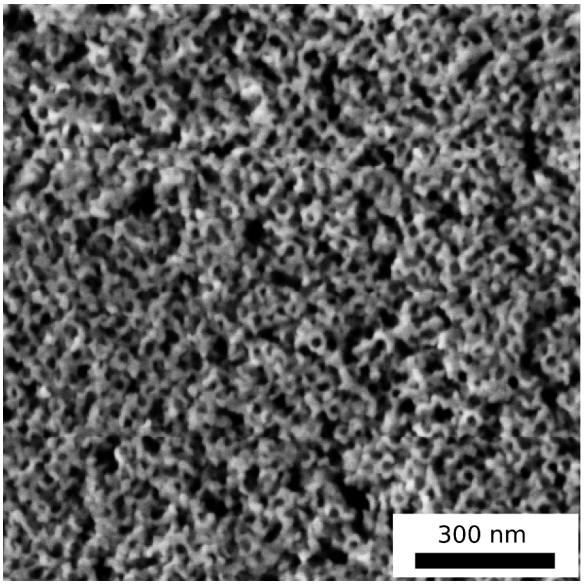

Figure S15. SEM micrograph of Ni deposited into the PI matrix pores of PI-*b*-PS-*b*-PPC-4 (Q^{230} core-shell double gyroid).

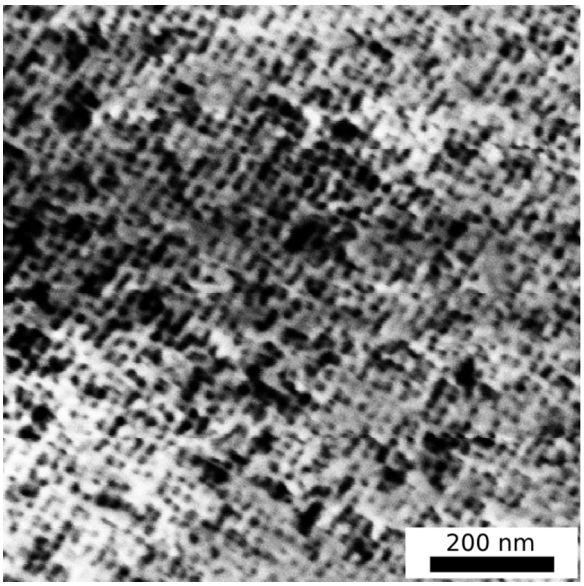

Figure S16. SEM micrograph of Ni deposited into the PPC minority network pores of PI-*b*-PS-*b*-PPC-1 (O^{70} orthorhombic network).

References

(1) Cohen, C. T.; Chu, T.; Coates, G. W. *J. Am. Chem. Soc.* **2005**, *127*, 10869–10878.

(2) Warren, S. C.; Disalvo, F. J.; Wiesner, U. *Nat. Mater.* **2007**, *6*, 156–161.

(3) Stefik, M.; Wang, S.; Hovden, R.; Sai, H.; Tate, M. W.; Muller, D. A.; Steiner, U.; Gruner, S. M.; Wiesner, U. *J. Mater. Chem.* **2012**, *22*, 1078–1087.

(4) Empower Materials Poly(alkylene carbonates) Typical Properties http://www.empowermaterials.com/products/technical-information/. Accessed December 5, 2014.

(5) Epps, T. H.; Cochran, E. W.; Bailey, T. S.; Waletzko, R. S.; Hardy, C. M.; Bates, F. S. *Macromolecules* **2004**, *37*, 8325–8341.

(6) Epps, T. H.; Cochran, E. W.; Hardy, C. M.; Bailey, T. S.; Waletzko, R. S.; Bates, F. S. *Macromolecules* **2004**, *37*, 7085–7088.

(7) Chatterjee, J.; Jain, S.; Bates, F. S. *Macromolecules* **2007**, *40*, 2882–2896.

(8) Hsueh, H.-Y.; Chen, H.-Y.; Hung, Y.-C.; Ling, Y.-C.; Gwo, S.; Ho, R.-M. *Adv. Mater.* **2013**, *25*, 1780–1786.

(9) Kulyk, N.; Cherevko, S.; Chung, C.-H. *Electrochim. Acta* **2012**, *59*, 179–185.

(10) Vukovic, I.; Punzhin, S.; Vukovic, Z.; Onck, P.; Hosson, J. T. M. De; ten Brinke, G. *ACS Nano* **2011**, *5*, 6339–6348.